Reprinted from:

THE JOURNAL OF CHEMICAL PHYSICS VOLUME 59, NUMBER 8 15 OCTOBER 1973

Optical pumping of molecules II. Relaxation studies*

R. E. Drullinger

Department of Chemistry, Columbia University, New York, New York 10027

National Bureau of Standards,† Boulder, Colorado 80302

R. N. Zare

Department of Chemistry, Columbia University, New York, New York 10027

(Received 11 April 1973)

The ($v'' = 3, J'' = 43$) level of Na_2 has been optically aligned using the 4880-Å line of a cw argon ion laser as a light source. The relaxation of this alignment is measured upon addition of foreign gas. In a low-pressure regime, where the mean free path exceeds the diameter of the light beam which both pumps and samples the alignment, the relaxation of the alignment versus pressure shows a "dog-leg shape" consisting of two linear regions. The first linear region corresponds to both elastic (velocity-changing) and inelastic (primarily rotational transfer) collisional relaxation whereas the second corresponds purely to inelastic collisional relaxation. The former process is dependent on the mode structure of the laser and shows saturation with increased pressure. In this low-pressure regime, the measured cross sections are shown to be lower bounds to the true cross sections and excitation by a multimode laser is shown to be inequivalent to excitation by a white light source when the width of the holes in the velocity distribution of the absorber molecules are nonoverlapping.

I. INTRODUCTION

Optical pumping consists of the transfer of order from a light beam to a material sample. The optical pumping technique is often used to polarize an atomic sample by altering the populations of some magnetic sublevels relative to others. This may be done in two ways that Happer[1] has called "repopulation pumping" and "depopulation pumping." Repopulation pumping occurs when certain ground-state sublevels are repopulated by spontaneous decay of excited states pumped by the light beam. In this pumping process, the ordering of the ground-state sublevels arises from the transfer of polarization from the excited-state sublevels. Depopulation pumping occurs when certain ground-state sublevels preferentially absorb light. In this photoselection process,[2] the ordering of the ground-state sublevels arises from the build-up of excess population in the weakly absorbing sublevels. Because of the multiplicity of radiative decay routes for the electronically excited states of molecules, depopulation pumping rather than repopulation pumping is expected to be in general the more efficient mechanism for achieving optical pumping of molecules.

In a previous paper,[3] hereafter referred to as I, we exploited the orientational dependence of the photoabsorption cross section to optically pump the Na_2 molecule, which occurs to a small extent in vapors of sodium. This was accomplished by using the intense 4880-Å line of the argon-ion laser to pump the ($v'' = 3$, $J'' = 43$) → ($v' = 6$, $J' = 43$) transition of the Na_2 $B\,^1\Pi_u - X\,^1\Sigma_g^+$ blue-green band system.[4,5] The establishment of molecular alignment[6] of the ($v'' = 3$, $J'' = 43$) level of the ground state was demonstrated by observing the decrease in the degree of polarization of the fluorescence with increasing laser intensity.

If the rate of depletion of certain ground-state sublevels is more rapid than the rate of collisional randomization, then the molecular sample will show a marked degree of order. Once it is possible to prepare significant samples of optically pumped molecules, then all the diverse experimental studies carried out on optically pumped atomic vapors[1] may also be performed on optically pumped molecular vapors. These experiments may be roughly divided into two classes: (1) structural studies, in which radiofrequency resonances are induced between neighboring levels of unequal population in order to determine their energy separations[7]; and (2) relaxation studies, in which the collision rate or the pumping rate is altered in order to determine how the molecular system adjusts to a new steady-state distribution of order (disorder).

We report here a continuation of the optical pumping studies started in I where the emphasis has been placed on observing the over-all relaxation mechanism and interpreting it in terms of competing microscopic energy transfer steps.

II. EXPERIMENTAL

The experimental setup[8] is essentially the same as in I. The 4880-Å line of a cw argon ion laser enters a cell of sodium vapor and the molecular fluorescence is observed at right angles to the

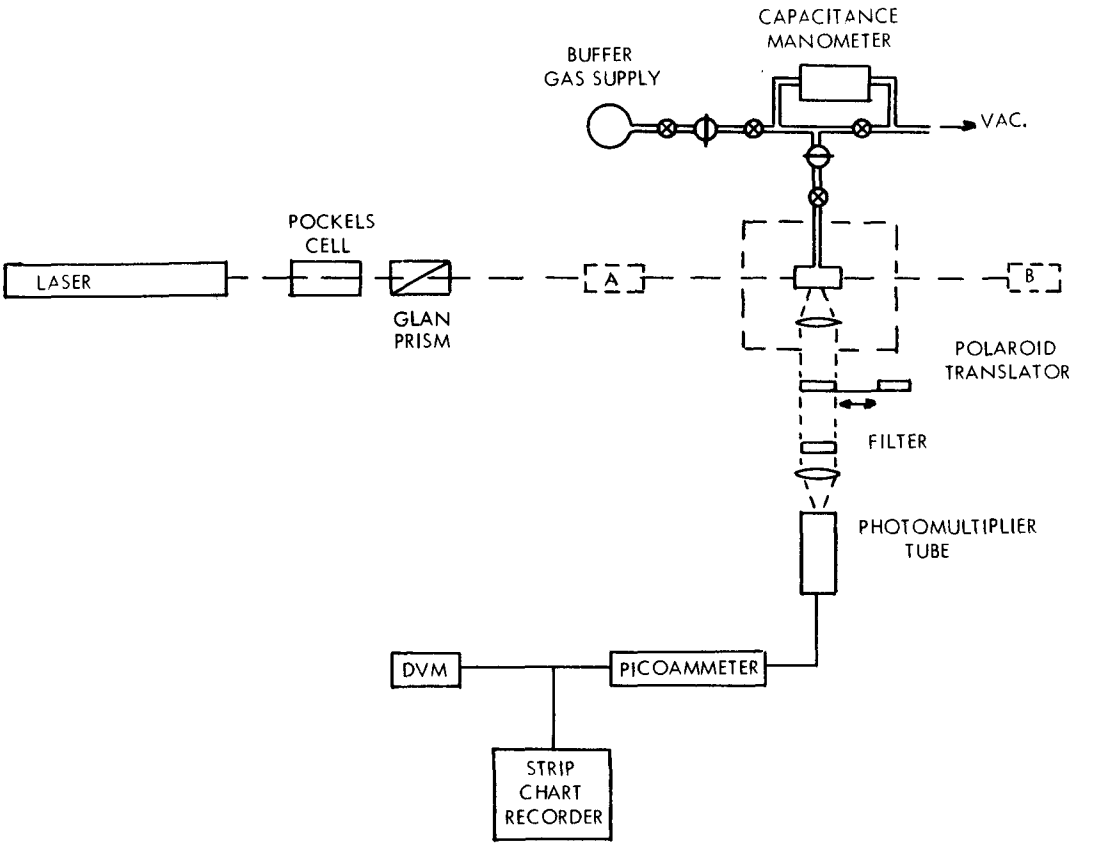

FIG. 1. Experimental setup for the measurement of the steady state degree of polarization as a function of foreign gas pressure.

laser beam. The intensity of the laser beam does not vary, as in I, but is maintained at some constant level while foreign gas is admitted to the cell. The Q-line progression originating from the $(v''=3, J''=43) \rightarrow (v'=6, J'=43)$ transition has a degree of polarization $P=50\%$ in the absence of foreign gas and in the limit of zero laser intensity (no optical pumping). The relaxation studies are carried out in the following manner. First, with no foreign gas present, the intensity of the laser beam is increased until the polarization of the fluorescence approaches $P=25\%$. As can be seen from Fig. 3 of I, in this operating region a change in the relaxation rate should result in the largest change in the degree of polarization. Second, foreign gas is added and the degree of polarization measured as a function of total cell pressure. Collisional relaxation rates are then deduced from the variation of the degree of polarization with foreign gas pressure.

Although the value of P is chosen to have maximum sensitivity at zero foreign gas pressure, the change of polarization over a large portion of an experimental run is only a few percent. Consequently, polarization measurements with a precision of a few parts in 10^4 are required in order to extract meaningful relaxation rates. This precision demanded that great care be taken with each element of the experimental setup; however, the final experimental arrangement, shown in Fig. 1, is quite simple.

The laser source must meet rather stringent noise and stability requirements. Although these requirements were not met by our home-built laser,[8] they are achieved with commercial laser systems that employ entirely solid-state power supplies. Two different commercial laser sources have been used successfully. Both produced identical results.

The plane-polarized laser beam first passes through a Pockels cell and Glan prism that are used in the determination of the time response of the system to sudden changes in the laser intensity (see below). The laser beam then passes through the cell, as shown in Fig. 1. Inside the cell the diameter of the laser beam is about 3 mm and the power is about 400 mW for $P=25\%$. The laser power is monitored alternately at positions A and

B in Fig. 1 so that the power level inside the cell can be maintained constant despite the gradual discoloration of the cell caused by alkali attack. This arrangement also permits the duty cycle of exposure time to off time of the cell to the laser beam to be maintained constant (see below).

As in I, the cell is 1 in. in diam, 3 in. long, and is constructed of Corning 1720 aluminosilicate glass, which resists alkali attack. The cell has a sidearm reservoir about 1 in. in length and $\frac{3}{8}$ in. in diam, which is maintained at a temperature a few degrees below that of the main body. Attached to the middle of the cell at right angles to both the cell and the reservoir, is another sidearm containing a stopcock. Through this sidearm foreign gas may be added or removed. At the point of attachment the walls are thickened to form a 1 cm long capillary with a 1 mm diam opening, thus minimizing the diffusion of the metal vapor into the cooler portions of the sidearm. A ground glass ball joint connects the sidearm to the gas-handling manifold.

The cell is placed on toroidal supports in an aluminum-block oven of the type illustrated in Fig. 2. The oven is a 4 in. $\times$4 in. $\times$6 in. block of aluminum, split lengthwise, with a $1\frac{1}{2}$ in. hole, bored its entire length, for housing the cell. A large conical section is bored into the base of the block to accommodate the alkali-metal reservoir. This allows the reservoir to remain about 1 °C cooler than the main body. Aluminum blocks at each end of the cell prevent the formation of cool spots on the oven windows. The fluorescence is viewed through a tapered elliptical section cut in the side of the oven. A sheet metal heat shield is placed around the cell for the twofold purpose of reducing heat loss through the fluorescence port and of acting as an aperture stop in the observation path so that off-axis fluorescence is suppressed. To further reduce heat loss and possible formation of local cool spots, a Pyrex window covers the fluorescence port. The oven is heated by means of No. 16 nichrome wire insulated by glass tubing and wound in grooves cut in the oven block. The entire aluminum block assembly is encased in a low-density firebrick. A large hole is bored in the firebrick to coincide with the fluorescence port and fitted with a lens, 3 in. in focal length. The lens forms part of the light collection optics and also provides additional heat baffling.

This system has a response time for temperature change of several hours and has proven stable to well within 0.1 °C. This high thermal stability is required in order that the number density of Na_2 molecules and Na atoms remains essentially constant during the course of a run. It is observed, however, that the cell temperature increases by as much as 0.25 °C when the laser beam is passed through the cell. The extent of the temperature change depends on the incident laser power and the amount of time that the cell is exposed to the laser beam. Consequently, the data have been obtained in a manner such that the duty cycle of exposure time to off time remains relatively constant.

The vacuum manifold is a simple glass system with greased stopcocks. Pressure measurements are made with a differential capacitance manometer referenced to the vacuum side of the manifold. All foreign gases used were research grade (99.95% pure or better).

The optics consist of a collimating lens, an analyzing polarizer, a narrow-band interference filter, and a focusing lens. The collimating lens is placed in the firebrick, as described above. The analyzing po[illegible] consists of a pair of

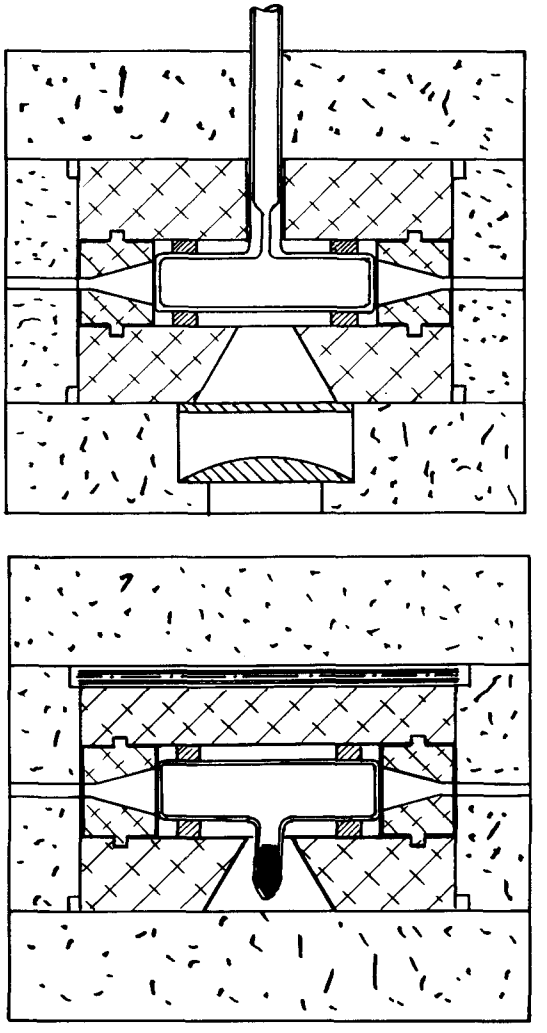

FIG. 2. Exposed view of the oven.

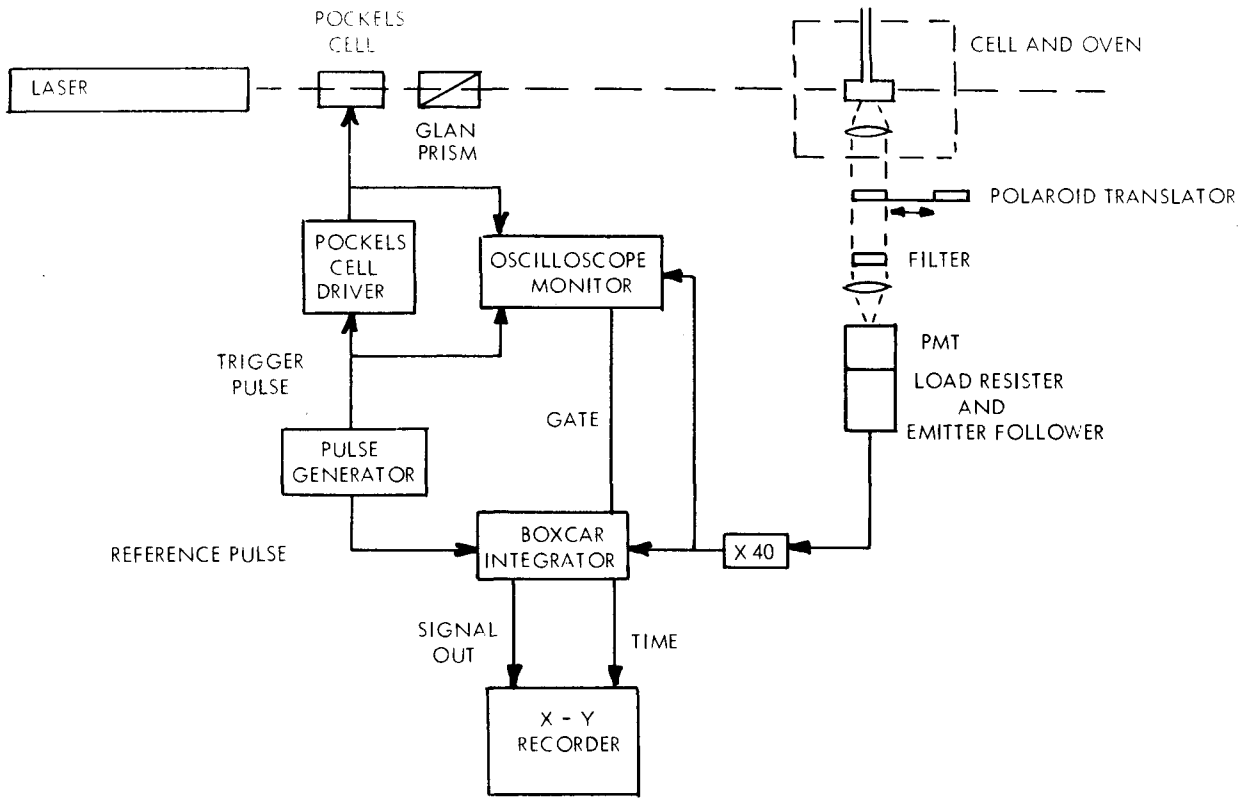

FIG. 3. Experimental setup for the measurement of the time response of a pumped system to the onset of pumping radiation.

matched Polaroid sheets mounted in a linear translator like that used for changing slides in a projector. With this arrangement the intensity components, $I_{\parallel}$ and $I_{\perp}$, that are parallel and perpendicular to the plane of polarization of the laser beam, respectively, are measured in a reproducible manner, even though the polarizer is hidden by light shielding. The interference filter was made commercially and has a transmission bandpass of 10 Å FWHM centered at 5250 Å. This filter allows the intense Q (13) line of the fluorescence progression (see Fig. 3 of Ref. 4) to pass with no detectable leakage of other nearby lines. The focusing lens images the fluorescence signal on the photocathode of the photomultiplier (EMI 6256 Å). The output of the photomultiplier is measured by a picoammeter that drives a digital voltmeter.

The degree of polarization P defined as

$$P=(I_{\parallel}-I_{\perp})/(I_{\parallel}+I_{\perp}) \tag{1}$$

is found by successively measuring $I_{\parallel}$ and $I_{\perp}$. The response of the entire detection system (optics and electronics) is calibrated by measuring its response to 0 and 100% polarized light. This measurement is accomplished by replacing the fluorescence cell with either a source of unpolarized light (a spinning light bulb) or a source of totally polarized light (a light bulb and a sheet of Polaroid).

For the purposes of placing the relaxation measurements on an absolute basis, it is necessary to determine the transient response of the pumped system to changes in the laser intensity. This was accomplished with the experimental setup shown in Fig. 3. A combination of a Pockels cell and Glan prism forms a fast shutter used to gate the laser beam on with a rise time of 100 nsec. The time response of the optical pumping signal (fluorescence) is sampled by a fast boxcar integrator and displayed on a XY recorder. For these measurements, the Pockels cell is required to have a step function response. Preliminary measurements encountered the difficulty that the Pockels cell exhibited piezoelectric ringing that modulated the light transmission. This was overcome by the use of an Isomet model 403A transverse-field light modulator.

III. DEVELOPMENT OF A PHENOMENOLOGICAL EXPRESSION FOR THE RELAXATION RATE

Optical pumping is a dynamic equilibrium in which the alignment of the sample by repeated encounters with the polarized, directional, and fre-

quency-selected photons of the light source is balanced by various relaxation processes that tend to restore the system to its initial distribution in the absence of irradiation by the light beam. In general, the relaxation is caused by a complex set of competing mechanisms, such as collisions of various kinds with other gas-phase species, collisions with the walls of the container, spatial diffusion of the optically pumped molecules in and out of the light beam, spontaneous radiative decay, etc. Often one relaxation mechanism will dominate the others under some set of operating conditions and the relaxation of the optically pumped sample than may be described in a simplified manner.

In the same spirit as one introduces the Bloch equations to describe the magnetic relaxation of ensembles of nuclei,[9] we introduced in I a master equation for the rate of change of the density of molecules $n(\theta, \varphi, t)$ in the pumped level having their transition dipoles pointing in the direction θ, φ at time t.

$$dn(\theta, \varphi, t)/dt = -\beta I n(\theta, \varphi, t)\cos^2\theta + \alpha[n_0 - n(\theta, \varphi, t)], \quad (2)$$

where we have introduced only one phenomenological parameter, α, to describe the rate at which the optically pumped sample is restored to its initial distribution n_0. In Eq. (2) $\beta I n(\theta, \varphi, t)\cos^2\theta$ represents the classical pumping rate[10] in which θ measures the angle between the polarization vector of the linearly polarized light beam and the axis of the transition dipole that coincides with the total angular momentum vector **J** for a $\Delta J = 0$ (Q-branch) transition.

As shown in I, the steady-state degree of polarization, defined as in Eq. (1), is found from Eq. (2) to have the form

$$P = [3\gamma(3\gamma^2+1)\tan^{-1}(\gamma^{-1}) - 9\gamma^2]/[3\gamma(\gamma+1)(\gamma-1)\tan^{-1}(\gamma^{-1}) - 3\gamma^2 + 4] \quad , \quad (3)$$

where

$$\gamma^2 = \alpha/\beta I \quad (4)$$

is the ratio of the relaxation rate coefficient to the pumping rate coefficient. Thus a measurement of P and βI permits a determination of the value of α.

In order to interpret the measurement of α, we must try to understand what processes constitute the relaxation mechanism. In the present experiment there are three basic channels by which the optically pumped sample may lose its alignment. First, the aligned molecules may suffer collisions that change their orientation, either randomly or in a gradual manner. Second, molecules from nearby (v'', J'') levels or molecules in the original (v'', J'') level but with velocity components that are not pumped may undergo collisions that transfer them into the pumped level. Finally, there is spatial diffusion in which unpumped molecules in the (v'', J'') level being pumped enter the laser beam while optically pumped molecules in the same level exit. To aid in the analysis of these relaxation mechanisms, we make the assumption that the optical pumping process affects only the population in the specific (v'', J'') level being pumped, and hence does not significantly alter the populations of nearby (v'', J'') levels from their equilibrium values. This assumption cannot be completely justified, but without much additional information (not at our disposal) we could not proceed. Furthermore, the reasonableness of this assumption is apparent if many levels "feed" the optically pumped level so that the effects of optical pumping are diluted among the feeder levels. We now discuss these three relaxation mechanisms in turn.

The magnetic sublevels M are degenerate in a field-free region. Consequently, collisions are always energetically capable of causing changes in the orientation of the molecule. Nevertheless, collisional reorientation seems to be a very minor relaxation process in our experiments for the following reasons. For large J values, the behavior of the diatomic molecule may be described as that of a spinning top. Small changes (i.e., $\Delta M = \pm 1$) in the top axis (taken to coincide with **J**) hardly change the degree of polarization of the molecular fluorescence.[5] For collisions to have sufficient torque to appreciably alter the direction of **J**, the magnitude of the angular rotation velocity appears to be altered as well, i.e., for molecules with rotational spacings less than kT, inelastic rotational transitions occur, contributing to the relaxation of the pumped system, but not by what we call collisional reorientation. This interpretation is further supported by several microwave–microwave double-resonance experiments that show that collisions between OCS molecules are ineffective in mixing M states for low J values.[11,12] In addition, we have investigated the depolarization of the $v' = 6$, $J' = 43$ level of the Na_2 $B\,^1\Pi_u$ state as a function of gas pressure. By observing the molecular fluorescence through a spectrometer that isolates the fluorescence from various upper-state levels, we find that pressures of about 10 torr (1 torr = 133.3 N/m^2) cause significant rotational transfer (observed by the presence of collision-induced satellite lines), but the depolarization of the parent level is *not* detectable. This last finding bears so directly on the reorientation relaxation of the $v'' = 3$, $J'' = 43$ level of the ground state that we feel justified in neglecting reorientation relaxation in what follows.

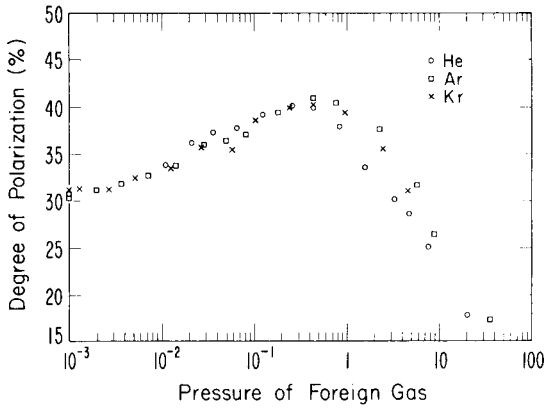

FIG. 4. Steady state degree of polarization as a function of foreign gas pressure (torr).

The frequency with which a molecule undergoes collisions of a specific type is given by $N\bar{v}\sigma$ where N is the number density of collision partners, $\bar{v} = (8kT/\pi\mu)^{1/2}$ is the mean relative velocity between the molecule under study and its collision partner, and σ is the effective (Maxwell–Boltzmann-averaged) cross section for this type of collision. Consider a molecule in the state (v_L, $v''=3$, $J''=43$) that is being pumped, where v_L is the velocity component of the molecule along the direction of the laser beam. The rate at which this molecule undergoes collisions that remove it from the state (v_L, $v''=3$, $J''=43$) is $N\bar{v}\sigma_T$, where σ_T represents the sum of cross sections for all types of collisions that take the molecule out of the state (v_L, v'', J'') being pumped. Then the rate at which $n(\theta, \varphi, t)$ is decreased by collisions is given by $N\bar{v}\sigma_T\, n(\theta, \varphi, t)$ where $n(\theta, \varphi, t)$ is the density of molecules in state (v_L, v'', J'') with dipoles directed into θ, φ. If the (v_L, v'', J'') level is not optically pumped, the population in this level will be at its equilibrium value, n_0, and the rate of collisional removal will be $N\bar{v}\sigma_T\, n_0$. At equilibrium, there is no net change in the population of this level. Thus the rate at which collisions bring molecules into the (v_L, v'', J'') level from other levels is also $N\bar{v}\sigma_T\, n_0$. Since we have assumed that optical pumping does not alter the population in levels other than the pumped level, the net rate of change of the population of pumped molecules caused by collision-induced transitions is $Nv\sigma_T[n_0 - n(\theta, \varphi, t)]$. Hence, the relaxation coefficient α depends on the pressure of foreign gas N through the term $N\sigma_T\bar{v}$.

Relaxation by spatial diffusion is an important process but the details of this process are not the goal of this study. By choosing to work in a pressure regime in which the mean free path greatly exceeds the light beam diameter, collisional diffusion effects may be ignored. Instead, we must take into account the rate at which unpumped molecules replace the pumped molecules in the laser beam (pumping-sampling region) through free flow. Let a^{-1} be the mean transit time for molecules to traverse the pumping region. Then the rate at which unpumped molecules in the (v_L, v'', J'') level enter the beam is $n_0 a$ and the rate at which pumped molecules leave the beam is $n(\theta, \varphi, t)a$. Thus spatial diffusion contributes a term $a[n_0 - n(\theta, \varphi, t)]$ to the relaxation rate, where a is independent of pressure in this low-pressure regime.

By combining the collision-induced transition processes with the spatial diffusion process, the phenomenological relaxation rate coefficient, α, may be rewritten as

$$\alpha = a + N\bar{v}\sigma_T \quad . \tag{5}$$

Thus the variation of α with foreign gas pressure N would be expected to be a straight line whose slope is the collision-induced relaxation rate $\bar{v}\sigma_T$ and whose intercept is the mean transit frequency a.

IV. RESULTS AND DISCUSSION

A. Gross Features

Figure 4 presents a plot of the degree of polarization P as a function of foreign gas pressure that illustrates the gross features that are expected from the collisional relaxation of a pumped system. At zero pressure, the degree of polarization is about one-half of the value it would have in the absence of optical pumping. In this plot alone, an enlarged laser beam was used to exemplify the transition from free flow to collisional diffusion. This prevented us from obtaining the power density necessary to produce an initial degree of pumping corresponding to 25% polarization. As gas is added to the cell, the polarization increases towards its value in an umpumped system, clearly indicating the presence of collisional relaxation. As the pressure is increased to a point where gas-kinetic collisions occur with a mean free path shorter than the diameter of the light beam [about 40 μ in this figure ($1\ \mu = 0.133\ \mathrm{N/m^2}$)], the effects of diffusion become apparent, and the degree of polarization shows an inverse pressure dependence that is characteristic of a diffusion-controlled rate. The inverse pressure dependence of this region is caused by the fact that the onset of diffusion slows the rate at which unpumped molecules enter the pumping-sampling region and pumped molecules leave it. This feature of the relaxation curve, which has the appearance of a dip or plateau, can be moved up and down the curve by decreasing or increasing the diameter of the light beam. With further increase in the foreign gas pressure, the collisional relaxation rate in the beam overcomes

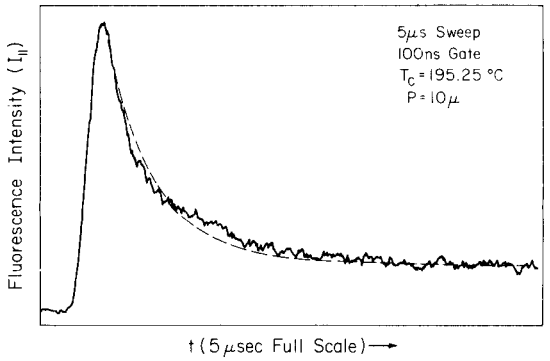

FIG. 5. Response of one polarization component of the fluorescence to the onset of pumping radiation.

the reduction in the rate at which molecules diffuse in and out of the beam so that the degree of polarization again increases towards its unpumped limit. However, at pressures of about 1 mm, the $v'=6$, $J'=43$ level of the excited state, having a lifetime of about 6 nsec,[5] begins to suffer collisions that cause transitions to neighboring rotational levels. These changes alter the apparent degree of polarization observed through the interference filter by mixing Q-line fluorescence (having a positive polarization) with P- and R-line fluorescence (having a negative polarization).[13] We choose to make careful collisional relaxation measurements in the low-pressure regime below the onset of diffusion.

B. Determination of the Pumping Rate

In order to extract α from the value of γ^2 deduced from the steady-state degree of polarization measurements, it is necessary to determine the pumping rate βI. This is accomplished by observing how the optically pumped system evolves in time following the onset of irradiation by the laser beam at time $t=0$. In Eq. (21) of I, we showed that the fluorescence intensity polarized parallel to the light beam had the time dependence

$$I_{\parallel}(t)=\int_0^{2\pi}\int_0^{\pi}(\cos^4\theta\, n_0/\gamma^2+\cos^2\theta)\{\gamma^2+\cos^2\theta \times\exp[-\beta I(\gamma^2+\cos^2\theta)t]\}\sin\theta d\theta d\varphi\ , \qquad (6)$$

where the derivation of this equation has neglected the variation in the spatial distribution of the intensity across the laser beam diameter. Figure 5 shows the time evolution of $I_{\parallel}(t)$. Also shown on this figure (dashed line) is the best nonlinear least squares fit to $I_{\parallel}(t)$ obtained from Eq. (6). This is accomplished by using the measured value of γ^2 (obtained on the same system from steady-state polarization measurements) and only one adjustable parameter, βI. The value of βI is found to be in this case

$$\beta I=2.47\times10^6\ \text{sec}^{-1}\ . \qquad (7)$$

The systematic error in βI caused by the assumption of a flat intensity profile of the laser beam is believed to be larger than any statistical or other instrumental errors associated with the determination of βI. The shape of the dashed curve shown in Fig. 5 is quite sensitive to the value of βI and the fact the fit using the functional form given in Eq. (6) is so good, encourages our belief in the phenomenological relaxation model. We estimate that βI is accurate to 10% based on the degree of fit. With this value of βI we can convert values of γ^2 to absolute values of the relaxation rate coefficient α. In particular, we find that the zero-pressure values of γ^2 and βI yield an α of $1.73\times10^5\ \text{sec}^{-1}$. This zero-pressure value of α corresponds to a, the mean transit frequency. It is interesting to note that if we crudely estimate a as the reciprocal transit time of a Na_2 molecule having the most probable velocity to traverse the diameter of the light beam, we find the same value of a to within 1%. The agreement is better than we have reason to expect but this further increases our confidence in the measurement of βI.

C. Low-Pressure Regime

Using the same experimental conditions, i.e., pump rate as in Sec. IV B, steady-state degree of polarization measurements are carried out for the foreign gases, He, Ne, Ar, Kr, Xe, H_2, D_2, N_2, and CH_4. The value of γ^2 is found from P by graphically inverting Eq. (3). We are then able to determine $\alpha=a+N\bar{v}\sigma_T$ for the different foreign gases, using the value of βI determined above.

Figure 6 illustrates typical data obtained in the low-pressure regime for collisional relaxation by argon. Two linear regions are apparent, one below and the other above 10 μ. Thus over this pressure region the relaxation mechanism changes in a most remarkable manner. The dog-leg appearance of Fig. 6 is characteristic of data in the low-pressure regime.

An appreciation of the first linear region requires an understanding of the frequency distribution of the laser light source.[14] Under the Doppler width of the laser transition, there is a frequency range, called the gain curve, for which stimulated emission exceeds the losses. This defines the gross width of the laser output. However, because the laser operates inside a resonant cavity of length L, only certain frequencies under the gain curve, called longitudinal modes satisfy the standing-wave boundary conditions. Typically, the laser runs multimode, i.e., consists of a group of lines spaced $c/2L$ apart whose intensities are determined by their positions under the gain curve. The modes are extremely narrow and not all the modes are active[15] at any instant. Because of plasma

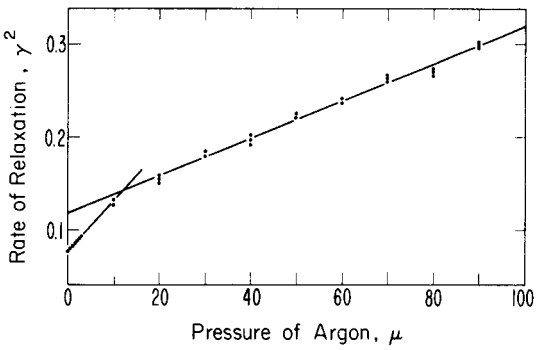

FIG. 6. Plot of the pumping parameter, γ^2, as a function of argon pressure.

and resonator instabilities, the modes jitter in frequency and the modes that are active change in time. On a long time scale, corresponding to the measurement of the mode structure with a Fabry–Perot interferometer, the modes appear to have an effective width for our laser of 50 MHz with a mode separation of about 130 MHz and a gross gain width of about 3000 MHz. On the shorter time scale that a molecule in a resonant (v_L, $v''=3$, $J''=43$) level is exposed to the laser beam, we are unable to define an effective mode width and unable to determine how many modes are active. Consequently, we do not know how to interpret this relaxation process in an accurate quantitative manner.

Nevertheless, only molecules with specific velocity components v_L will be able to absorb the laser light (i.e., only those molecules whose Doppler shifted resonant frequency equals one of the laser modes). Consequently, the laser pumps only certain velocity components v_L of the ($v''=3$, $J''=43$) level. Elastic collisions contribute to the relaxation process by transfering molecules within the ($v''=3$, $J''=43$) level from unpumped velocity components to velocities resonant with the laser modes.

We note that this relaxation mechanism saturates as a function of pressure. With increasing foreign gas pressure a point is reached where all velocity components are mixed rapidly compared to the time a ($v''=3$, $J''=43$) molecule spends in the laser beam. At this point, the relaxation caused by velocity-changing collisions no longer increases with increasing pressure. This type of relaxation is related to the relaxation observed in hole-burning experiments when foreign gas is added.[16–18]

To confirm that the first linear region is dominated by velocity-changing collisions, we repeated the same measurements using different laser mode spacing, as shown in Fig. 7. Here helium is used as the foreign gas. In Fig. 7(a) the mode spacing is about 65 MHz; in Fig. 7(b) the mode spacing is about 130 MHz; while in Fig. 7(c), the laser is operated single mode so that only one mode is active. As the mode spacing approaches the width of the holes in the velocity distribution, the number of molecules within the ($v''=3$, $J''=43$) level having the necessary velocity component to absorb the laser radiation approaches the total number of molecules in the ($v''=3$, $J''=43$) level. Thus, as expected, Fig. 7 shows that the magnitude of the relaxation, as indicated by the difference between the intercepts of the first and second linear regions, increases with increasing mode spacing.[19] Figure 7 also shows that the breakpoint where saturation of the mechanism occurs, appears to be relatively independent of the mode structure of the laser while the slope in the first linear region changes little between Fig. 7(a) and 7(b). This implies that most velocity-changing collisions produce small increments in the velocity component along the laser beam. If the collisions distributed molecules in the pumped (v'', J'') level uniformly over the Maxwellian velocity distribution, then the slope of the first linear region would increase as the mode spacing increased since less of the molecules entering a given pumped velocity distribution ("hole") would have originated from regions already pumped. The similarity in slopes in the first linear region therefore leads us to conclude that at least for He collision partners a "strong-collision" model[16] is inappropriate for describing the velocity relaxation of pumped Na_2 molecules.

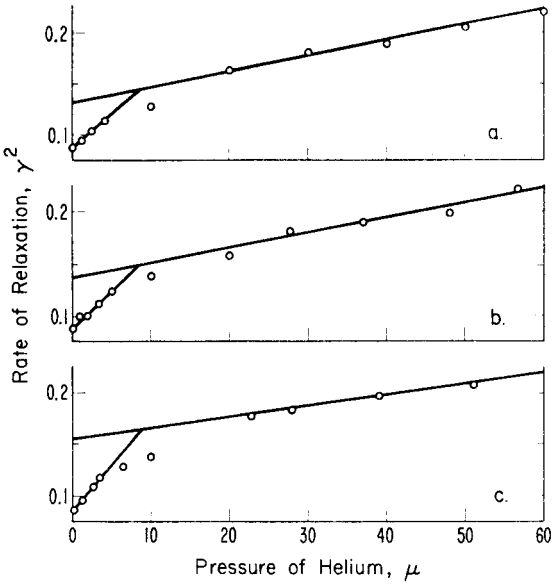

FIG. 7. Effect of laser cavity mode separation on the relaxation plots: (a) 65 MHz mode spacing, (b) 130 MHz mode spacing, and (c) single mode operation.

TABLE I. Effective cross sections[a] for relaxing the optically pumped ($v''=3$, $J''=43$) level of Na_2 through elastic collisions (σ_{El}) and through inelastic collisions (σ_{In}).

Foreign gas	σ_{El} (Å^2)	σ_{In} (Å^2)
He	39 ± 3	14 ± 1
Ne	50 ± 5	22 ± 1
Ar	59 ± 2	35 ± 1
Kr	84 ± 10	39 ± 2
Xe	84 ± 17	45 ± 2
H_2	49 ± 4	12 ± 1
D_2	62 ± 2	16 ± 2
CH_4	70 ± 9	30 ± 2
N_2	94 ± 12	41 ± 2

[a]The errors quoted are the statistical errors only and represent one standard deviation.

The second linear region, as shown in Figs. 6 and 7, corresponds to inelastic collisional relaxation whereby molecules are transferred in and out of the (v'', J'') pumped level. The inelastic processes responsible for this transfer are a sum of rotational and vibrational collisional-induced transitions. Because rotational transfer within the same vibrational state has a cross section much larger than transfer from other rotational levels of different vibrational states,[20] it is reasonable to assume that the second linear region represents primarily inelastic rotational relaxation. Since the first linear region is the sum of relaxation rates caused by the inelastic collisions and elastic, velocity-changing collisions, the elastic relaxation rate is found by subtracting the inelastic relaxation rate, given by the slope of the first linear region.

We have ignored collisions that cause ΔM changes in the pumped (v'', J'') level, and have argued previously that such reorientation relaxation should be quite minor because large ΔM changes within a (v'', J'') level are rare. It might be wondered whether successive ΔM changes of small magnitude, e.g., $\Delta M=\pm 1$, might contribute to the relaxation rate. Relaxation by successive collisions would lead to a nonlinear dependence of the relaxation rate on the pressure. However, the linearity of our relaxation data, as indicated in Fig. 6, causes us to dismiss this mechanism.

D. Effective Cross Sections

Cross sections for the different foreign gases are obtained from the slopes of the relaxation versus pressure plots, similar to those shown in Figs. 6 and 7, by multiplying the slope (found by a least squares fit) by the factor $\beta I/\bar{v}$. The results are presented in Table I. The interpretation of σ_T as a cross section requires some qualification. Let $P(b)$ be the probability that a collision of a certain kind will take place with an impact parameter b for a certain relative velocity. Then the cross section for the collision process is given by integrating over all impact parameters

$$\sigma = \pi \int_0^\infty P(b)\, b^2 db \tag{8}$$

and then averaging σ over all relative velocities. Calculations often show that for cross sections larger than gas kinetic cross sections, $\sigma_{gk}=\pi b_{gk}^2$, impact parameters less than b_{gk} contribute about as much to the cross section as those impact parameters greater than b_{gk}. However, by the nature of our experiment, we discriminate against collisions with small impact parameters since in the low-pressure regime, the mean free path for hard (gas kinetic) collisions is larger than the diameter of the laser beam. This means that a molecule will most likely travel through the laser beam before suffering a small impact parameter collision. For example, a molecule has a mean free path approximately given by $(\pi b^2 N)^{-1}$ for collision with impact parameter b [we assume b is small so that $P(b)\sim 1$]. If this mean free path is greater than the laser beam diameter, the effect of these collisions will not be reflected in the observed relaxation rate and hence our measured cross sections will be smaller than the quantity σ defined by Eq. (8). For a pressure of 10^{-2} torr and a laser beam diameter of 3 mm, this argument shows that collisions with impact parameters less than 5 Å are discriminated against and hence the measured cross sections can be significantly altered by this effect at low pressures. However, at 1 torr pressure only collisions with impact parameters $b<0.5$ Å are discriminated against and the effect should be much smaller. Thus collisions with impact parameters b less than the impact parameter b_{cutoff} corresponding to the mean free path equal to the mean transit distance of the beam are weighted by some factor less than b^2db in contributing to the observed collisional relaxation. Consequently, the effective cross sections given in Table I are lower bounds to the true cross section.

Bergmann and Demtröder[20] have measured rotational cross sections for the B $^1\Pi_u$ state of Na_2, which has a larger internuclear equilibrium separation than the ground state by about 15%. They find typical total rotational inelastic cross sections of about 60 Å^2. Our effective cross sections are lower by a factor of 2 to 3. This could be influenced by the fact that we are measuring a ground state σ which should be somewhat smaller in any case.

Elastic cross sections are typically hundreds of

square angstroms in size for the alkali dimers.[21] While from Table I σ_{E1} is about twice as large as σ_{In}, it is not of this magnitude. However, the value for σ_{E1} has been decreased from the true elastic cross section by the effect mentioned above and by the lack of resolution caused by the velocity hole as a velocity-change detector (analogous to the loss of resolution caused by the finite detector size in elastic scattering experiments[22]). Here the resolution is reduced by the width of the hole burned in the velocity distribution of molecules in the pumped (v'', J'') level.

For many purposes, it is convenient to regard laser sources as extremely bright light bulbs with highly monochromatic output and to ignore the details of their output frequency distribution. For the optical pumping of molecules, however, we have found that the laser pumps only molecules with certain velocity components and thus the relaxation depends on the details of the laser mode structure.[23] These primitive relaxation studies show that this technique has the ability of separating elastic from inelastic collision processes. Because of power limitations, much of this work was carried out in a low-pressure regime where the mean free path exceeds the laser diameter. This causes the effective cross sections to be lower bounds to the true cross sections. However, with presently available commercial laser systems it is possible to extend these relaxation studies into the region above the onset of diffusion. This should allow the extraction of more meaningful collision cross sections.

ACKNOWLEDGMENTS

We thank P. Pechukas and E. W. Smith for critically reading a first draft of this paper and for making many useful comments.

*Support from the National Science Foundation is gratefully acknowledged.

†Present address.

[1]W. Happer, Rev. Mod. Phys. **44**, 169 (1972).

[2]A. C. Albrecht, J. Mol. Spectrosc. **6**, 84 (1961); R. Bersohn and S. H. Lin, Adv. Chem. Phys. **16**, 67 (1969).

[3]R. E. Drullinger and R. N. Zare, J. Chem. Phys. **51**, 5532 (1969).

[4]W. Demtröder, M. McClintock, and R. N. Zare, J. Chem. Phys. **51**, 5495 (1969).

[5]M. McClintock, W. Demtröder, and R. N. Zare, J. Chem. Phys. **51**, 5509 (1969).

[6]In our studies we use only linearly polarized light so that the optically pumped sample may become "aligned," but not "oriented." By alignment we mean that the $+M$ and $-M$ magnetic sublevels are equally populated, but the different $|M|$ sublevels vary in population.

[7]See for example, Robert W. Field, Robert S. Bradford, David O. Harris, and H. P. Broida, J. Chem. Phys. **56**, 4712 (1972), in which we believe the ground state optical-microwave double resonance measurements are facilitated by optical pumping of one of the levels by irradiation with a cw argon ion laser.

[8]For additional information, see R. E. Drullinger, Ph.D. thesis, Columbia University, New York, 1972 (University Microfilms, Order Number 73-9011, Ann Arbor, Michigan).

[9]F. Block, Phys. Rev. **70**, 460 (1946).

[10]A quantum treatment for the master rate equation also has been developed in I. However, as discussed in I, for large J values the quantum expression cannot be distinguished from the classical expression, which is much easier to use.

[11]A. P. Cox, G. W. Flynn, and E. B. Wilson, Jr., J. Chem. Phys. **42**, 3094 (1965).

[12]M. L. Unland and W. H. Flygare, J. Chem. Phys. **45**, 2421 (1966).

[13]R. N. Zare, J. Chem. Phys. **45**, 4510 (1966).

[14]See C. K. N. Patel, *Lasers*, edited by A. K. Levine (Dekker, New York, 1968), Vol. 2, pp. 1–190.

[15]C. G. B. Garrett, *Gas Lasers*, (McGraw-Hill, New York, 1967) and references cited therein.

[16]P. W. Smith and T. Hänsch, Phys. Rev. Lett. **26**, 740 (1971).

[17]J. L. Hall, "The Lineshape Problem in Laser-Saturated Molecular Absorption" in *Lectures in Theoretical Physics*, edited by K. T. Mahanthappa and W. E. Britton, Jr. (Gordon and Breach, New York, 1969).

[18]W. Demtröder, "Spectroscopy with Lasers" in *Topics in Current Chemistry* (Springer, Berlin, 1971), Vol. 17.

[19]An attempt was made to observe how the relaxation rate changed when the frequency of the single mode laser was varied, i.e., when different velocity components in the direction of the laser beam were pumped. However, the sensitivity of our experiment proved insufficient to distinguish any effect.

[20]K. Bergmann and W. Demtröder, J. Phys. B **5**, 2098 (1972).

[21]P. Rosenberg, Phys. Rev. **55**, 1267 (1939); Phys. Rev. **57**, 561 (1940).

[22]P. Kusch, J. Chem. Phys. **44**, 1 (1964).

[23]For a recent examination of this topic, particularly as it relates to the optical pumping of atoms in magnetic fields, Phys. Rev. A 8, 1844 (1973).